

Light, electron microscopy and DNA sequences of the dinoflagellate *Prorocentrum concavum* (syn. *P. arabianum*) with special emphasis on the periflagellar area

NORMAWATY MOHAMMAD-NOOR, ØJVIND MOESTRUP AND NIELS DAUGBJERG*

Section of Phycology, Department of Biology, University of Copenhagen, Øster Farimagsgade 2D,
DK-1353 Copenhagen K, Denmark

N. MOHAMMAD-NOOR, Ø. MOESTRUP AND N. DAUGBJERG. 2007. Light, electron microscopy and DNA sequences of the dinoflagellate *Prorocentrum concavum* (syn. *P. arabianum*) with special emphasis on the periflagellar area. *Phycologia* 46: 549–564. DOI: 10.2216/06-94.1

We have reexamined the original culture of *Prorocentrum arabianum* Morton et Faust (CCMP 1724) using a combination of light and electron microscopy in addition to gene sequence data. Compared to the original description of *P. arabianum* (Morton *et al.* 2002), the new observations revealed it to possess two pyrenoids surrounded by starch sheaths and two types of valve pores, but marginal pores were absent. Cells kept in culture for nearly a decade now appeared symmetrical to asymmetrical in outline rather than asymmetrical as in the original description. In culture, *P. arabianum* attached to the bottom of culture flasks instead of being an active swimmer. Also in culture it produced large amounts of mucus. Studying serial sectioned cells in the transmission electron microscope, the periflagellar area was seen to comprise nine platelets. The overall arrangement of platelets agreed with Taylor's scheme from 1980 except for one additional plate labeled a2 situated between a1, b and e. Further ultrastructural examination of *P. arabianum* revealed for the first time a connection between a pusule-like organelle surrounded by two membranes and the accessory pore within the periflagellar area. We speculate that the pusule canal is used for discharging mucus or particulate matter through the accessory pore. The LSU rDNA sequence divergence between *P. arabianum* and *P. concavum* isolated from Malaysia was only 0.2%. As such a low divergence value is usually seen only at the population level, we also determined nuclear-encoded ITS 1 and ITS 2 and the cytochrome *b* (*cob*) gene residing in the mitochondrial genome in the two taxa. These DNA fragments were identical (ITS 1 and ITS 2) or almost identical (cytochrome *b*) when comparing *P. arabianum* and *P. concavum*. Amalgamating all available information from ultrastructure and molecular data, we conclude that *P. arabianum* is a synonym of *P. concavum*. It should, however, be noted that there is a difference in toxin profile between the two isolates. A phylogeny based on partial LSU rDNA including 14 species of *Prorocentrum* and 40 other dinoflagellates indicated that the genus may comprise six groups, and each of these are supported by a combination of morphological features and toxin production. As statistical support from bootstrap values or posterior probabilities for the divergent branches in the LSU tree was low, we refrain from major systematic changes of the genus *Prorocentrum* until more species are examined in the electron microscope and new DNA fragments other than ribosomal genes become available.

KEY WORDS: LSU rDNA phylogeny, Periflagellar area, *Prorocentrum arabianum*, *Prorocentrum concavum*, *Prorocentrum faustiae*, Ultrastructure

INTRODUCTION

The genus *Prorocentrum* was first erected by Ehrenberg in 1834 with *P. micans* as the type species. Since then, numerous species have been described primarily from marine environments (e.g. Loeblich *et al.* 1979; Fukuyo 1981; Faust 1990, 1997; Ten-Hage *et al.* 2000b). However, two species are known from freshwater/brackish water (Croome & Tyler 1987). Studies on *Prorocentrum* have grown in number after many of the newly described species were shown to produce toxins (e.g. Murakami *et al.* 1982; Morton 1998; Morton *et al.* 1998; Denardou-Queneherve *et al.* 1999; Ten-Hage *et al.* 2000a; Holmes *et al.* 2001) with potentially adverse effects on human health (Ten-Hage *et al.* 2000a, 2002). A precise identification based on a complete description is needed to prevent misidentification with closely allied species. *Prorocentrum arabianum* Morton & Faust was first described from the Gulf of Oman based on light and scanning electron microscopy (SEM)

and reported to produce cytotoxic and ichthyotoxic compounds (Morton *et al.* 2002). Since this species is morphologically similar to *P. concavum* Fukuyo and *P. faustiae* Morton, a thorough description using light, electron microscopy (SEM and transmission electron microscopy [TEM]) and DNA sequences is needed. From a phylogenetic viewpoint, a more complete study on *Prorocentrum* is important to test the hypothesis by McLachlan *et al.* (1997) that the genus *Prorocentrum* be split and the genus *Exuviaella* be reinstated. The characters supporting separation of *Exuviaella* were its primarily benthic habitat, its absence of an obvious apical spine or tooth, its presence of mucocysts and production of DSP-type toxins. Few studies have so far contradicted the suggestion by McLachlan *et al.* (1997) (Morton 1998; Puigserver & Zingone 2002; Pearce & Hallegraef 2004), probably because more *Prorocentrum* species have to be examined before the taxonomy of *Prorocentrum* can be further assessed.

Studies on the ultrastructure of *Prorocentrum* are few compared to the number of species identified. The number of platelets in the periflagellar area has been suggested by

* Corresponding author (nielsd@bi.ku.dk).

Table 1. List of dinoflagellates and ciliates (outgroup) included in the phylogenetic analyses. Strain numbers and GenBank accession numbers are also provided. — = information not available.

Species	Strain numbers	GenBank accession numbers for LSU rDNA
<i>Akashiwo sanguinea</i> (Hirasaka) Gert Hansen & Moestrup	JL36	AF260396
<i>Alexandrium affine</i> (Inouye & Fukuyo) Balech	—	AY294612
<i>Alexandrium margalefii</i> Balech	—	AY154957
<i>Amphidinium gibbosum</i> (Maranda & Shimizu) Flø Jørgensen & Murray	SI-36-50	AY460587
<i>Baldinia anauniensis</i> Gert Hansen & Daugbjerg	—	EF052683
<i>Ceratium fusus</i> (Ehrenberg) Dujardin	—	AF206390
<i>Ceratium lineatum</i> (Ehrenberg) Cleve	—	AF260391
<i>Dinophysis acuminata</i> Claparède & Lachmann	—	AY277640
<i>Dinophysis acuta</i> Ehrenberg	—	AY277648
<i>Dinophysis norvegica</i> Claparède & Lachmann	—	AY571375
<i>Esoptrodinium gemma</i> P. Javornický	—	DQ289020
<i>Gonyaulax baltica</i> Ellegaard, Lewis & Harding	UW394	AY154962
<i>Gonyaulax membranacea</i> (Rossignol) Ellegaard, Daugbjerg, Rochon, Lewis & Harding	UW398	AY154965
<i>Gymnodinium catenatum</i> L.W. Graham	—	AF200672
<i>Gymnodinium fuscum</i> (Ehrenberg) Stein	CCMP1677	AF200676
<i>Gymnodinium impudicum</i> (Fraga & Bravo) Gert Hansen & Moestrup	JL30	AF200674
<i>Gymnodinium nolleri</i> Ellegaard & Moestrup	K-0602	AF200673
<i>Gyrodinium dominans</i> Hulbert	—	AY571370
<i>Gyrodinium rubrum</i> (Kofoid & Swezy) Takano & Horiguchi	—	AY571369
<i>Gyrodinium spirale</i> (Bergh) Kofoid & Swezy	—	AY571371
<i>Heterocapsa arctica</i> Horiguchi	CCMP 445	AY571372
<i>Heterocapsa rotundata</i> (Lohman) Gert Hansen	K-0479	AF260400
<i>Heterocapsa triquetra</i> (Ehrenberg) Stein	K-0447	AF260401
<i>Jadwigia applanata</i> Moestrup, Lindberg & Daugbjerg	CCAC 0021	AY950447
<i>Karenia brevis</i> (Davis) Gert Hansen & Moestrup	JL32	AF200677
<i>Karenia mikimotoi</i> (Miyake & Kominani ex Oda) Gert Hansen & Moestrup	—	AF200681
<i>Karlodinium armiger</i> Bergholtz, Daugbjerg & Moestrup	K-0668	DQ114467
<i>Karlodinium veneficum</i> (Ballantine) J. Larsen	Plymouth 103	DQ114466
<i>Kryptoperidinium foliaceum</i> (Stein) Lindemann	K-0638	EF052684
<i>Lepidodinium chlorophorum</i> (Elbrächter & Schnepf) Gert Hansen, Botes & de Salas	K-0539	AF200669
<i>Peridiniella catenata</i> (Levander) Balech	K-0543	AF260398
<i>Peridinium willei</i> Huitfeldt-Kaas	AJC2-675	AF260384
<i>Pfiesteria piscicida</i> Steidinger & Burkholder	—	AY112746
<i>Polarella glacialis</i> Montresor, Procaccini, Stoecker	—	AY571373
<i>Prorocentrum arabianum</i> Morton & Faust ¹	CCMP 1724	EF566752
<i>Prorocentrum arenarium</i> Faust	K-0625	EF566747
<i>Prorocentrum cf. faustiae</i> Morton	NMN013	EF566744
<i>Prorocentrum concavum</i> Fukuyo	NMN08	EF566751
<i>Prorocentrum donghaiense</i> Lu	—	AY822610
<i>Prorocentrum emarginatum</i> Fukuyo	PES401	EF566750
<i>Prorocentrum lima</i> (Ehrenberg) Dodge	NMN07	EF566748
<i>Prorocentrum micans</i> Ehrenberg	K-0335	AF260377
<i>Prorocentrum minimum</i> (Pavillard) Schiller	K-0010	AF260379
<i>Prorocentrum playfairi</i> Croome & P.A. Tyler	—	—
<i>Prorocentrum rhathymum</i> Loeblich, Sherley & Schmidt	NMN16	EF566745
<i>Prorocentrum rhathymum</i>	JL35	AF260378
<i>Prorocentrum sculptile</i> Faust	NMN011	EF566749
<i>Prorocentrum sigmoides</i> Bohm	—	EF566746
<i>Prorocentrum foveolata</i> Croome & P.A. Tyler	—	—
<i>Scrippsiella cf. hangoei</i> (J. Schiller) J. Larsen	K-0399	AF260392
<i>Scrippsiella trochoidea</i> var. <i>aciculifera</i> Montresor	K-0500	AF260393
<i>Tovellia coronata</i> (Woloszynska) Moestrup, Lindberg & Daugbjerg	B1	AY950445
<i>Tovellia sanguinea</i> Moestrup, Gert Hansen, Daugbjerg, Flaim & D'Andrea	—	DQ320627
<i>Woloszynskia pseudopalustris</i> (Woloszyńska) Kiselev	AJC12cl-915	AF260402
<i>Woloszynskia tenuissima</i> (Lauterborn) Moestrup, Gert Hansen et Daugbjerg	—	AY571374
Ciliate outgroup		
<i>Spathidium amphoriforme</i> Greeff	—	AF223570
<i>Tetrahymena pyriformis</i> (Ehrenberg) Lwoff	GL-C	X54004
<i>Tetrahymena thermophila</i> Nanney & McCoy	B1868VII	X54512

¹ A synonym of *P. concavum* but kept here as *P. arabianum*.

Taylor (1980) to be of systematic importance, and it has been used as one of the characters to identify *Prorocentrum* species (e.g. Faust 1993a, b, 1994, 1997; Ten-Hage *et al.* 2000a; Hoppnath 2000). To obtain an accurate number

and configuration of the platelets present, TEM is a superior but time-consuming technique. Few studies have used TEM (Faust 1974; Loeblich 1976) whereas SEM is widely used (e.g. Faust 1993a, b, 1997; Morton 1998; Ten-Hage *et al.*

2000b). Occasionally, light microscopy has been used (Fukuyo 1981), sometimes based on silver stained material (Biecheler 1952). Considering the minute size of the platelets, determination of the number of platelets by SEM and light microscopy is difficult and may result in wrong interpretations.

The existence of two pores in the periflagellar area of *Prorocentrum* has long been recognized (e.g. Biecheler 1952; Parke & Ballantine 1957) and also that these differ in size (Faust 1974; Zhou & Fritz 1993). The larger pore is the flagellar pore through which the two flagella emerge (Loeblich *et al.* 1979; Honsell & Talarico 1985; Zhou & Fritz 1993; Roberts *et al.* 1995). The emerging of both flagella from a single pore was found early on by Schütt (1896), but subsequently it was suggested, incorrectly, that the two flagella exit through individual pores (Bursa 1959; Dodge & Bibby 1973; Loeblich 1976) as in other dinoflagellates. The smaller pore is known by several names, such as auxiliary pore (e.g. Faust 1993a, b, 1997; Morton 1998), apical pore (Zhou & Fritz 1993) and accessory pore (Fensome *et al.* 1993; Roberts *et al.* 1995). The function of this pore remains unknown.

A well-developed pusule is usually present in dinoflagellates. The term 'pusule' was first introduced by Schütt (1895) to describe a vacuole thought to function as a contractile vacuole as in other flagellates, although Schütt never saw any contractions. Since then, the pusule has been an object of interest, but its function is still controversial. Several functions have been suggested, such as fluid intake (Kofoid & Swezy 1921), osmoregulation (Dodge 1972), macromolecule uptake, secretion (Klut *et al.* 1987) or an entry or exit route for liquid and particulate matter (Calado *et al.* 1999). However, in *Prorocentrum*, studies on the pusule are few.

In this study we have attempted to fill in some of the gaps in our knowledge of *Prorocentrum* by reexamining the original culture of *P. arabianum* Morton & Faust, which is still available from the Provasoli-Guillard National Collection for Culture of Marine Phytoplankton as strain CCMP 1724. We have applied light, epifluorescence and electron microscopy in addition to sequence determination of nuclear-encoded large subunit ribosomal DNA (LSU rDNA), internal transcribed spacer 1 and 2 (ITS 1 and ITS 2), and mitochondrial cytochrome *b* (*cob*). The periflagellar area is examined in detail, including the number of platelets and the possible role of the accessory pore.

MATERIAL AND METHODS

Algal cultures

A culture of *P. arabianum* (CCMP 1724) was obtained from the Provasoli-Guillard National Collection for Culture of Marine Phytoplankton, USA. The culture was grown in L1 medium (Guillard & Hargraves 1993). Cells of *P. concavum* (strain NMN08) and *P. cf. faustiae* (strain NMN013) were isolated from seagrass and *Sargassum* sp. collected in Sabah, Malaysia, and grown in ES-DK medium (Kokinos & Anderson 1995). Both species were grown at 26–27°C in a 12:12 hr light:dark regime with a photon flux rate of 30 $\mu\text{mol photons m}^{-2} \text{s}^{-1}$.

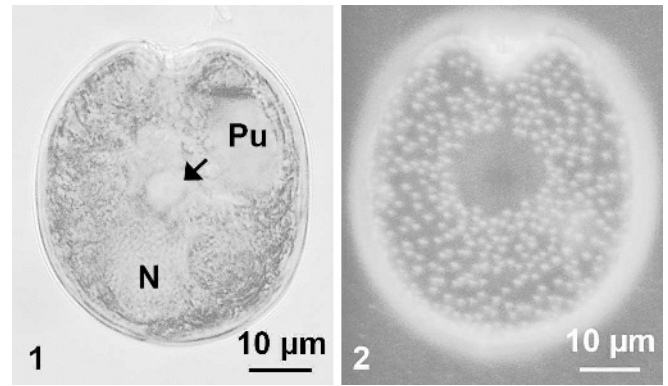


Fig. 1. Light microscopy of *Prorocentrum concavum* (syn. *P. arabianum*, CCMP 1724) showing one of two central pyrenoids (arrow), the dorsal nucleus (N) and the pusule (Pu). Anterior view. **Fig. 2.** Epifluorescence microscopy with Calcofluor White-stained cell showing valve pores except in the centre of the cell. Posterior view.

Light microscopy

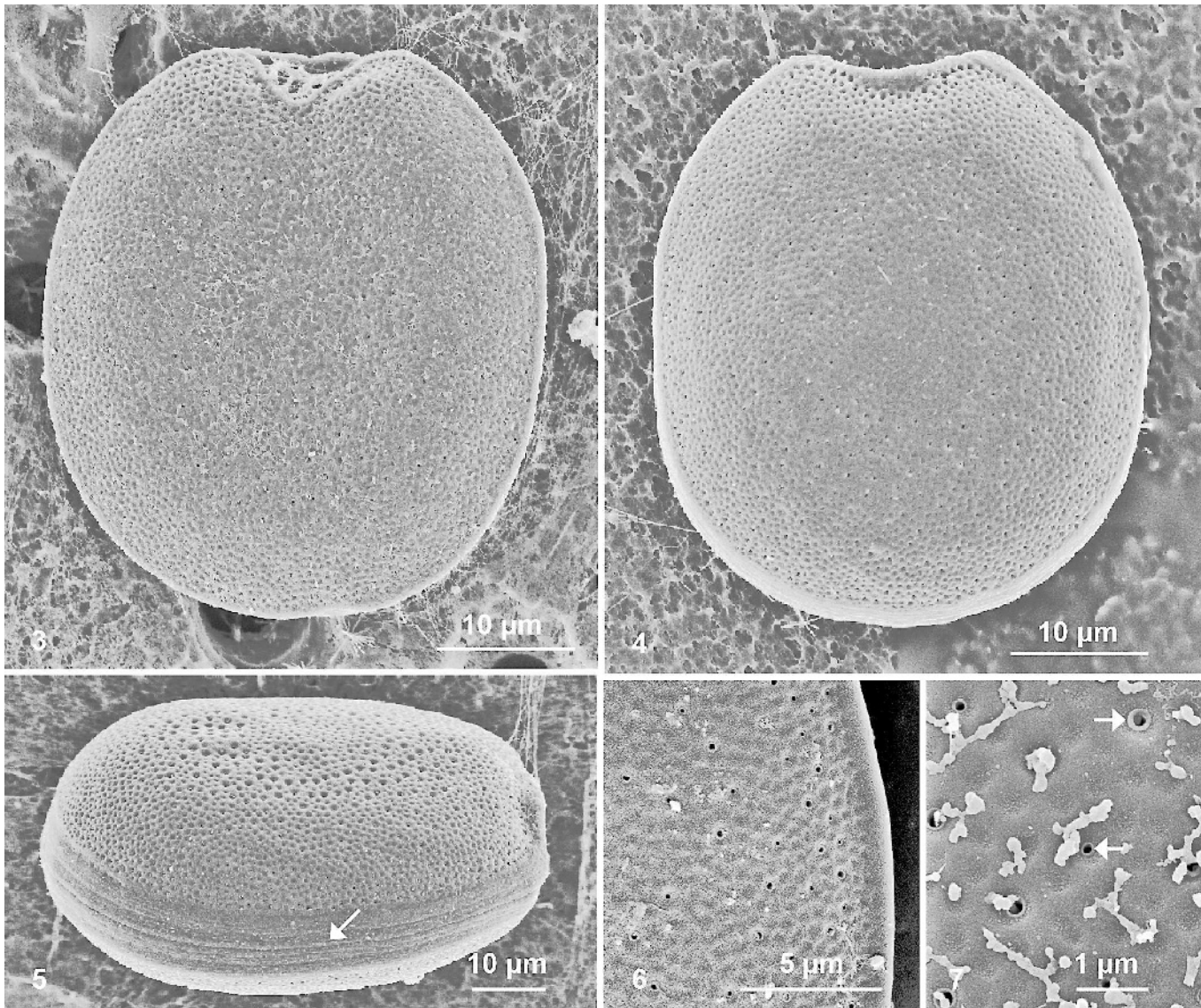
Cells were observed using an Olympus BX 60 light microscope equipped with differential interference contrast. Micrographs were taken with an Olympus digital camera DP10 (Tokyo, Japan). For visualization of valve pores, cells were stained with Calcofluor White (5 mg ml⁻¹; Sigma) (Fritz & Triemer 1985) and observed under violet light (405-nm excitation and 420-nm emission). Cell dimensions were determined using an eyepiece micrometer at $\times 400$ magnification. Morphometrics were based on measurements of 20 cells.

Scanning electron microscopy

Live samples in growth medium were fixed at room temperature for ~ 1 h in 1% OsO₄, rinsed in distilled water for 1 h to remove salt and fixatives, dehydrated in a graded series of ethanol (30, 50, 70, 96, 99.9 and 99.9% with molecular sieves), critical-point dried (CPD 030, BAL-TEC, Liechtenstein) and coated with a layer of platinum-palladium. Micrographs were taken on a JEOL JSM-6335F field emission scanning electron microscope (JEOL Ltd, Tokyo, Japan). The sizes of the valve pores were determined from scanning electron micrographs at $\times 10,000$ magnification of at least five cells as recommended by Faust (1991).

Transmission electron microscopy

The cultures were fixed for 1.5 h with 2% glutaraldehyde in 0.1 M cacodylate buffer containing 0.5 M sucrose at room temperature. Cells were concentrated at 2000 rpm for 10 min, and the supernatant was discarded. The supernatant was replaced with 0.1 M cacodylate buffer containing 0.25 M sucrose, followed by 0.1 M cacodylate buffer containing 0.12 M sucrose and 0.1 M cacodylate buffer, 20 min in each change. They were postfixed in 1% OsO₄ in 0.1 M cacodylate buffer overnight at 4°C. The cells were then rinsed briefly in distilled water and dehydrated at 4°C in a series of ethanols (15, 30, 50, 70 and 96%)



Figs 3–7. Scanning electron microscopy of *Prorocentrum concavum* (syn. *P. arabianum*, CCMP 1724).

Figs 3–5. The thecal surface is rugose and valve pores are evenly distributed except at the centre of each thecal plate.

Fig. 3. Posterior view showing that the cell shape is slightly asymmetrical and widely elongate, and the periflagellar area is wide and V-shaped.

Fig. 4. Anterior view showing cell shape, which is broadly elongate, and the ventral concave end.

Fig. 5. Side view showing horizontally striated intercalary band (arrow).

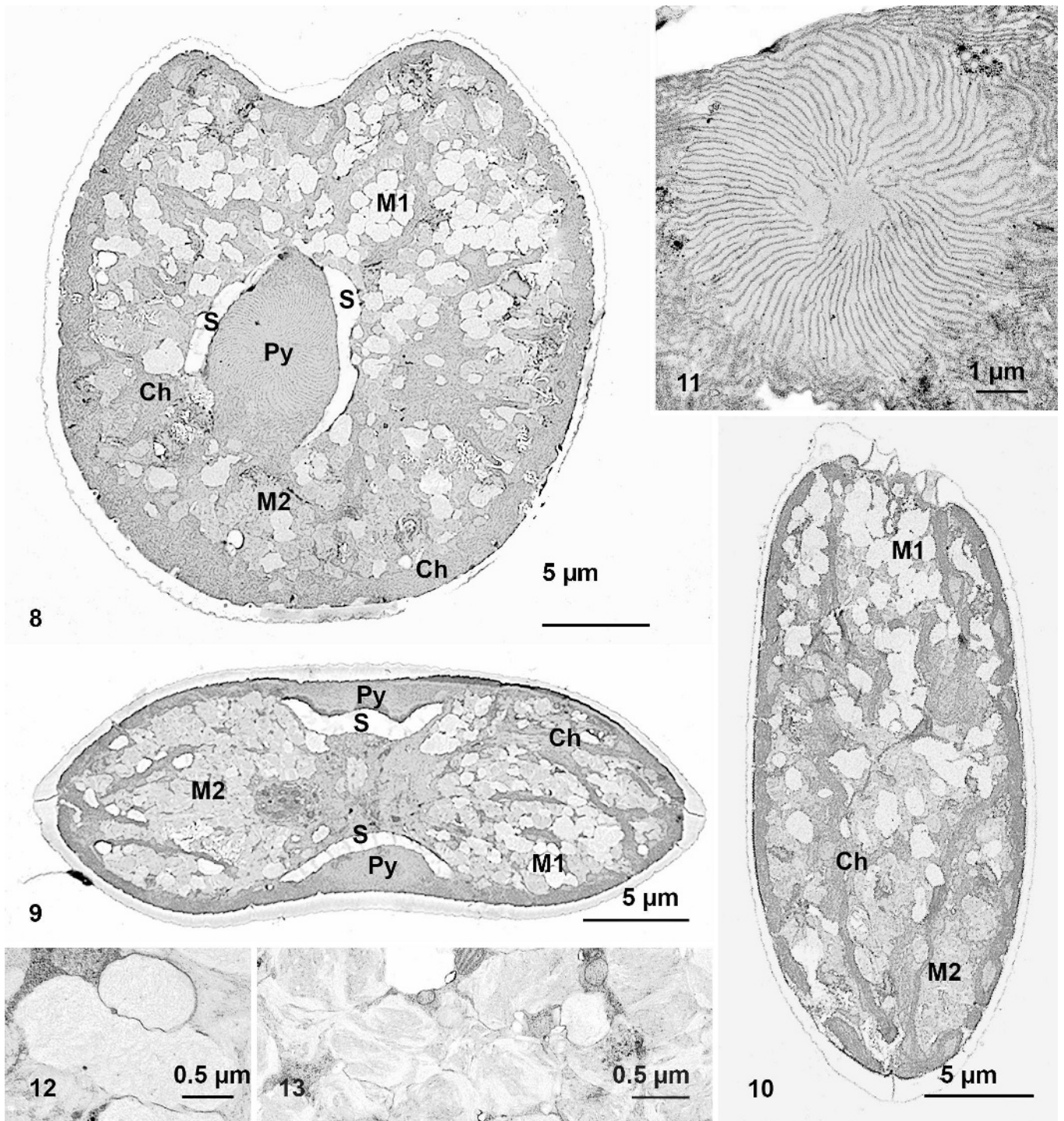
Fig. 6. Marginal pores are absent.

Fig. 7. Two different sizes of valve pores, each pore encircled by a ring-like structure (arrows).

followed by two changes of 99% ethanol at room temperature, 15 min in each step. The cells were transferred to 100% acetone for 5 min and then to 100% acetone/Spurr's resin (1:1) and the material was then left uncovered overnight at room temperature. The following morning cells were transferred to 100% Spurr's resin (two changes), 4 h in each change. Polymerization was at 75°C for at least 8 h. Thin sections were cut on an LKB Ultratome V ultramicrotome, collected on slot grids and stained for 20 min in aqueous uranyl acetate, followed by 20 min in lead citrate. The sections were examined in a JEM-1010 (JEOL Ltd) transmission electron microscope.

PCR amplification and sequence determination of *P. arabianum*, *P. cf. faustiae* and *P. concavum*

Exponentially growing cells of *P. concavum* were harvested by centrifugation at 1500 rpm at 15°C for 20 min. Total genomic DNA was extracted using the CTAB method (Doyle & Doyle 1987). Extracted DNA was used as template in a 0.5-ml thin-wall Eppendorf PCR tube together with PCR reagent (5 μl 10× Taq buffer, 0.67 M Tris/HCL pH 8.5, 0.02 M MgCl₂, 0.166 M [NH₄]₂SO₄, 0.1 M 2-mercaptoethanol), 20 μl 0.5 μM dNTP mix, 1 U Taq polymerase, 5 μl 10 μM of each primer, 5 μl 100 mM TMA (tetramethyl-ammonium chloride). Thermal cycles



Figs 8–10. General ultrastructure of *Prorocentrum concavum* (syn. *P. arabianum*, CCMP 1724).

Fig. 8. Transverse section through a valve showing central pyrenoid (Py) with starch sheath (S), chloroplasts (Ch) and two types of mucus vesicles (M1 and M2).

Fig. 9. Longitudinal section through both valves showing the two central pyrenoids (Py) with starch sheaths (S), chloroplasts (Ch) and mucus vesicles (M1 and M2).

Fig. 10. Longitudinal section showing chloroplasts (Ch) and mucus vesicles (M1 and M2).

Fig. 11. Pyrenoid with thylakoids radiating towards the pyrenoid centre.

Fig. 12. Mucus vesicles (M1) containing fibrous material.

Fig. 13. Mucus vesicles (M2) containing more opaque fibrous material.

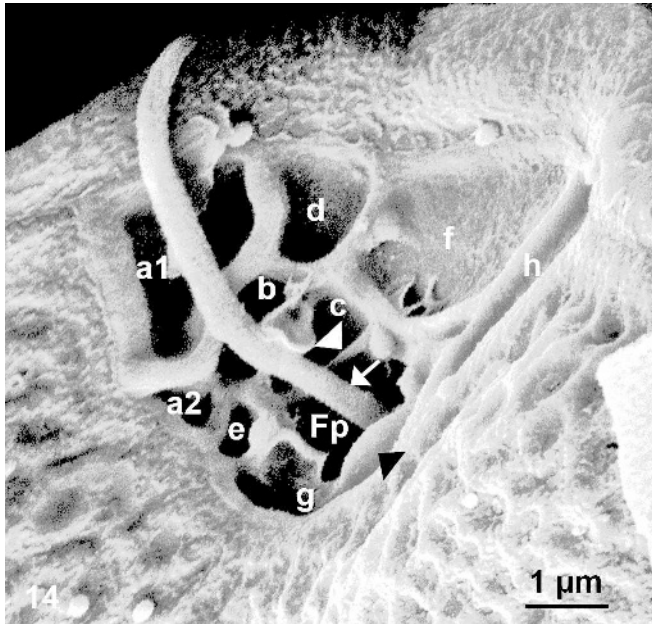


Fig. 14. Scanning electron microscopy of the periflagellar area in *Prorocentrum concavum* (syn. *P. arabianum*, CCMP 1724). Oblique posterior view showing platelets and flagellar pore (Fp), which is partly surrounded by a small flange (arrowheads). The longitudinal flagellum (arrow) exits through this pore. The accessory pore is hidden behind the flagellum.

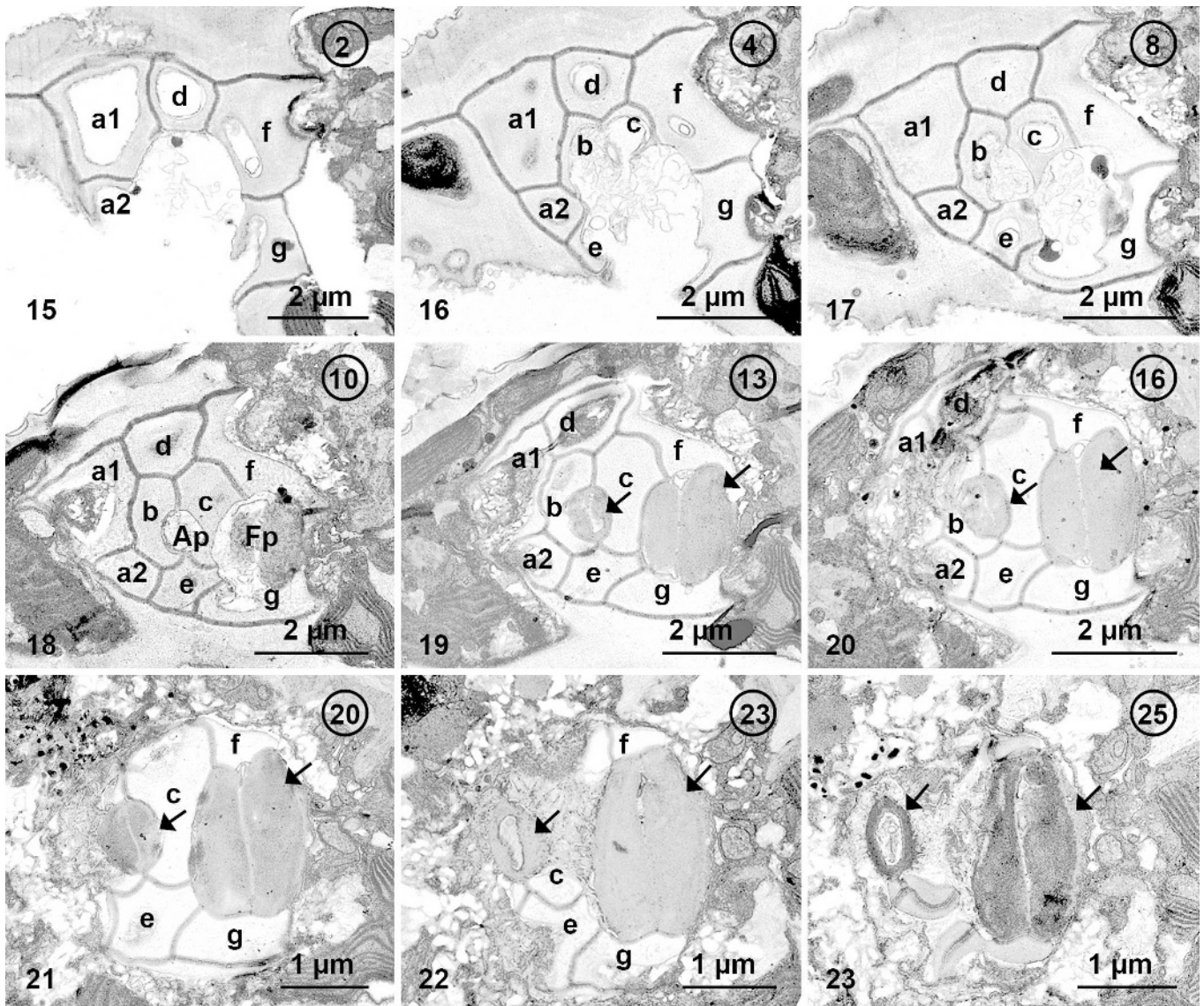
were run as follows: one initial denaturing step at 94°C for 3 min, followed by 35 cycles each consisting of 94°C for 1 min, 52°C for 1 min, and 72°C for 2 min and a final elongation cycle of 72°C for 6 min. Two cells from clonal cultures of *P. arabianum* (CCMP 1724) and *P. cf. faustiae* were isolated using capillary pipettes and washed individually three times in sterile double-distilled water before transfer to 0.5-ml thin-wall Eppendorf PCR tubes each containing 8 μ l sterile ddH₂O. The two cells were mixed with the PCR reagents described previously but without 1 U Taq polymerase and were heated for 10 min at 94°C using a PCR machine. Following this treatment, 1 U Taq polymerase was added to each tube, and thermal cycles were run as described previously. Two primers, D1R (forward) and 'Dino-specific' (reverse), were used to amplify approximately 1800 base pairs of the nuclear-encoded LSU rDNA gene (for primer sequences, see Scholin *et al.* 1994; Hansen & Daugbjerg 2004). The mitochondrial cytochrome *b* (cob) gene was amplified using primers Dinocob1F (forward) and Dinocob1R (reverse) (Zhang *et al.* 2005), and for rDNA-ITS regions, primers ITS 1F (5'-TCCGTAGGTGAACCTGCG-3') and ITS 4R (5'-TCCTCCGCTTATTGATATGC-3') were used (White *et al.* 1990). The temperature profiles for cob and ITS PCR reactions, respectively, were identical to that used for PCR of LSU rDNA. PCR fragments were electrophoresed on a 2% Nusieve agarose gel with EtBr and checked on a UV light table. PCR-amplified fragments of correct length were purified using the QIAquick PCR purification kit (Qiagen, Hilden, Germany) following the recommendations of the manufacturer. Purified PCR products (~ 20 ng μ l⁻¹) were

used in 20- μ l PCR reactions using the dye termination cycle sequencing ready reaction kit (PerkinElmer, Foster City, California) as suggested by the manufacturer. Sequencing reactions were run on an ABI 3100 Genetic Analyzer. The partial LSU rDNA sequences in both directions were obtained using terminal primer D1F in addition to internal primers D2C, D3A, D3B and ND1483R (for primer sequences, see Daugbjerg *et al.* 2000). The cob and ITS sequences were determined with the same primers used to amplify these DNA fragments in the PCR reactions.

Sequence alignment and phylogenetic analyses

The three partial LSU rDNA sequences determined were added to an alignment comprising 52 other dinoflagellates as listed in Table 1. Three ciliates (*Tetrahymena pyriformis*, *T. thermophila* and *Spathidium amphoriforme*) were included for outgroup rooting. The LSU rDNA sequences were aligned by incorporating information from the secondary structure as suggested by de Rijk *et al.* (2000) and further edited by eye using SeaView (Galtier *et al.* 1996). The data matrix comprised a total of 1499 base pairs, but because of ambiguous alignment of the highly variable domain D2 (*sensu* Lenaers *et al.* 1989), this fragment was excluded from the phylogenetic inferences. Hence, a total of 1149 base pairs were included in maximum parsimony (MP), neighbor-joining (NJ) and Bayesian analyses using PAUP* 4b10 (Swofford 2003) and MrBayes ver. 3.1 (Ronquist & Huelsenbeck 2003), respectively. For MP, 1000 random additions were performed using the heuristic search option and a branch-swapping algorithm (TBR) in PAUP. Characters were unordered and weighted equally. Introduced gaps were treated as missing data. Parsimony bootstrap analyses included 1000 replications. We used Modeltest ver. 3.7 by Posada & Crandell (1998) to find the best-fit model for the LSU rDNA data matrix, and the program suggested the TrN+I+G model as the best. Among sites, rate heterogeneity was $\alpha = 0.6583$, an estimated proportion of invariable sites was $I = 0.2482$ and two substitution rate categories were A-G = 2.517 and C-T = 6.6889. Base frequencies were set as follows: A = 0.2882, C = 0.1705, G = 0.2774 and T = 0.2639. The settings from this model were applied in NJ to compute dissimilarity values, and these were then used as input to build an NJ tree. NJ bootstrap analyses with the Modeltest maximum likelihood settings were performed with 1000 replications.

The GTR substitution model was invoked in Bayesian analysis with base frequencies and a substitution rate matrix estimated from the data. Four simultaneous Monte Carlo Markov chains (Yang & Rannala 1997) were run from random trees for 1×10^6 generations (Metropolis-coupled MCMC). A tree was sampled every 50 generations, and the 'burn-in' was estimated for stationarity by examination of the plateau in log likelihoods as a function of generations using a spreadsheet. The 'burn-in' of the chains occurred in fewer than 12,050 generations. Hence, the first 241 trees were discarded, and this left 19,760 trees for estimating posterior probabilities. Posterior probability values were obtained from a 50% majority rule consensus of the saved trees.



Figs 15–23. Selected sections from a series of sections through the periflagellar area of *Prorocentrum concavum* (syn. *P. arabianum*, CCMP 1724). The direction of sectioning is from ventral towards dorsal. Small encircled numbers refer to the section number. The platelets are joined together by prominent sutures. Platelet h is absent in these sections.

Fig. 15. Platelets a1, d and f are concave; therefore, only parts of the plates are visible.

Figs 16–17. Platelets b, c, e and g appear. Platelets b, c and e are also concave.

Fig. 18. The flagellar pore (Fp) and accessory pore (Ap) are both visible; the accessory pore is almost circular, while the flagellar pore is elongate.

Figs 19–22. Two elongated sac-like structures surround both the flagellar pore and the accessory pore (arrows).

Fig. 23. Almost all platelets have disappeared (this section is 23 sections away from the section in Fig. 15) leaving only the sac-like structures (arrows).

RESULTS

Morphology

We have adopted the terminology suggested by Schütt (1896) and Roberts *et al.* (1995) to describe cell orientation. Therefore, we use the term ‘ventral’ for the position where the flagella emerge, ‘dorsal’ for the opposite end, anterior valve for the largest valve and posterior valve for the smallest valve, that is, the valve with the indentation from which the flagella extend.

Prorocentrum arabianum is a photosynthetic dinoflagellate with golden-brown chloroplasts, two central pyrenoids and a dorsal nucleus (Fig. 1). The cells are symmetrical to asymmetrical, and elongate in valve view (Figs 1–4). The dorsoventral cell size ranges from 38 to 49 μm ($46 \pm 2.5 \mu\text{m}$), and the width is 35–40 μm ($38 \pm 2.0 \mu\text{m}$) ($n = 20$). These cell dimensions are slightly larger than those provided at the CCMP home page (<http://ccmp.bigelow.org>). The posterior valve is convex and the anterior valve concave (Fig. 9). The thecal surface is rugose (Figs 3–5) and ornamented with two different pore sizes (Fig. 7)

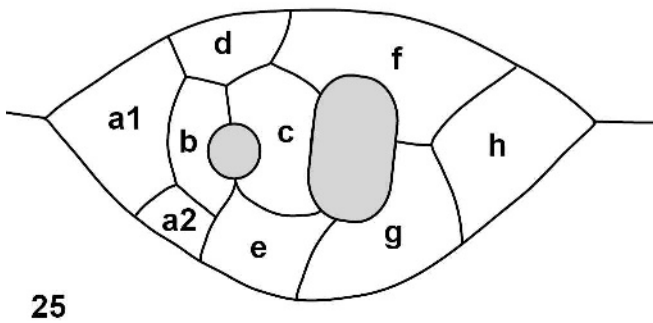
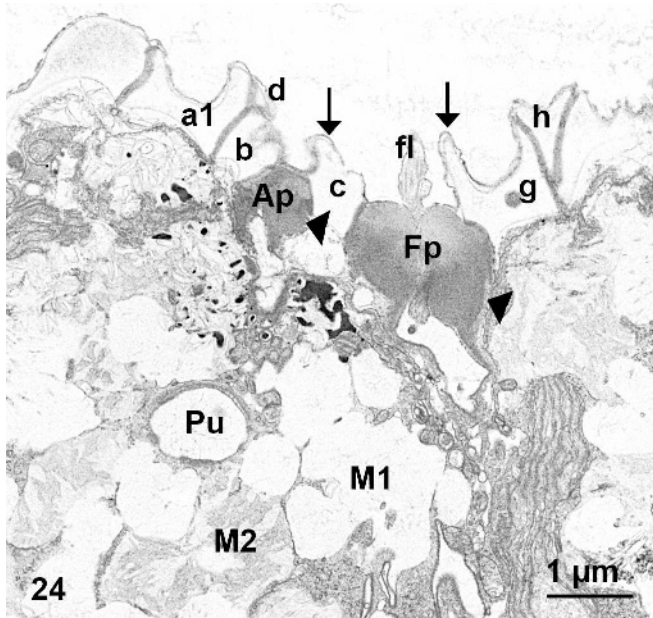


Fig. 24. The periflagellar area of *Prorocentrum concavum* (syn. *P. arabianum*, CCMP 1724) including both the flagellar pore (Fp), the accessory pore (Ap), two sac-like structures surrounding both pores (arrowheads), a flagellum (fl), platelets of the periflagellar area, small flanges extending from platelets g and c (arrows), the pusule (Pu) and the two types of mucus vesicles (M1 and M2).

Fig. 25. Diagrammatic reconstruction of the periflagellar area of *Prorocentrum concavum* (syn. *P. arabianum*, CCMP 1724) based on transmission electron microscopy, showing nine platelets together with the elongate flagellar pore and the circular accessory pore. Ventral view. Not to scale.

except centrally (Figs 2–4). Both pore types are located in shallow depressions, each encircled by a ring-like structure (Figs 6, 7). The pore diameter ranges from 0.17 to 0.21 μm ($0.19 \pm 0.01 \mu\text{m}$) for the large pores and from 0.10 to 0.13 μm ($0.12 \pm 0.01 \mu\text{m}$) for the smaller pores. The intercalary band is horizontally striated (Fig. 5). Marginal pores are absent (Fig. 6).

Swimming behaviour

Under our culture conditions, *P. arabianum* did not swim actively like other planktonic *Prorocentrum* species. Instead, cells often attached to the bottom of the culture flask, where they produced large amounts of mucus.

General ultrastructure

The main organelles are illustrated in a transverse section (Fig. 8) and two longitudinal sections (Figs 9, 10). The chloroplasts are positioned peripherally and radiate toward the cell centre (Figs 8–10). The two pyrenoids are located midway along the valves and surrounded by starch sheaths (Figs 8, 9). Pairs of thylakoids extend towards the pyrenoid centre (Fig. 11). Two types of vesicles, probably mucus vesicles, are observed throughout the cells (Figs 8–10). Both types, M1 in Fig. 12 and M2 in Fig. 13, contain fibrous material, but the material in M2 is more opaque. Trichocysts are absent (Figs 8–10).

Periflagellar area

As in other species of *Prorocentrum*, the periflagellar area is covered with platelets and penetrated by two pores, usually known as the flagellar and auxiliary pore (accessory or apical pore) (Fig. 14). The platelet area is lined by a prominent suture, forming a wide triangular periflagellar area (Fig. 14). Sutures between platelets are elevated and form indentations of the periflagellar area (Figs 14–17). No obvious ornamentation, such as spines or flanges, are visible except for small flanges surrounding part of the flagellar pore (Figs 14, 24). These small flanges are extensions of platelets c and g (Fig. 24). Figures 15–23 illustrate a series of sections through the periflagellar area to provide details of platelets and pores. In this series, nine platelets may be recognized (Figs 15–23, 25), and two sac-like structures surround each pore (Figs 15–25). The platelets are located on the posterior valve (Figs 14–17). The flagellar pore is much larger than the accessory pore (Figs 18–25), and both flagella exit through the flagellar pore (Figs 14, 24). For comparison, the platelets have been labelled according to Taylor’s scheme (Taylor 1980). The arrangement of the platelets agrees with this scheme except for the presence of one extra platelet, a2, between platelets a1, b and e (Figs 14–25). Four platelets (a, d, f and h) border the anterior valve (Figs 14–19, 25). The flagellar pore is surrounded by four platelets labelled c, e, f and g, while the accessory pore is surrounded by only two platelets, b and c (Figs 14–22, 24, 25). Platelet h does not touch the flagellar pore (Figs 14, 24, 25). The pores are separated from each

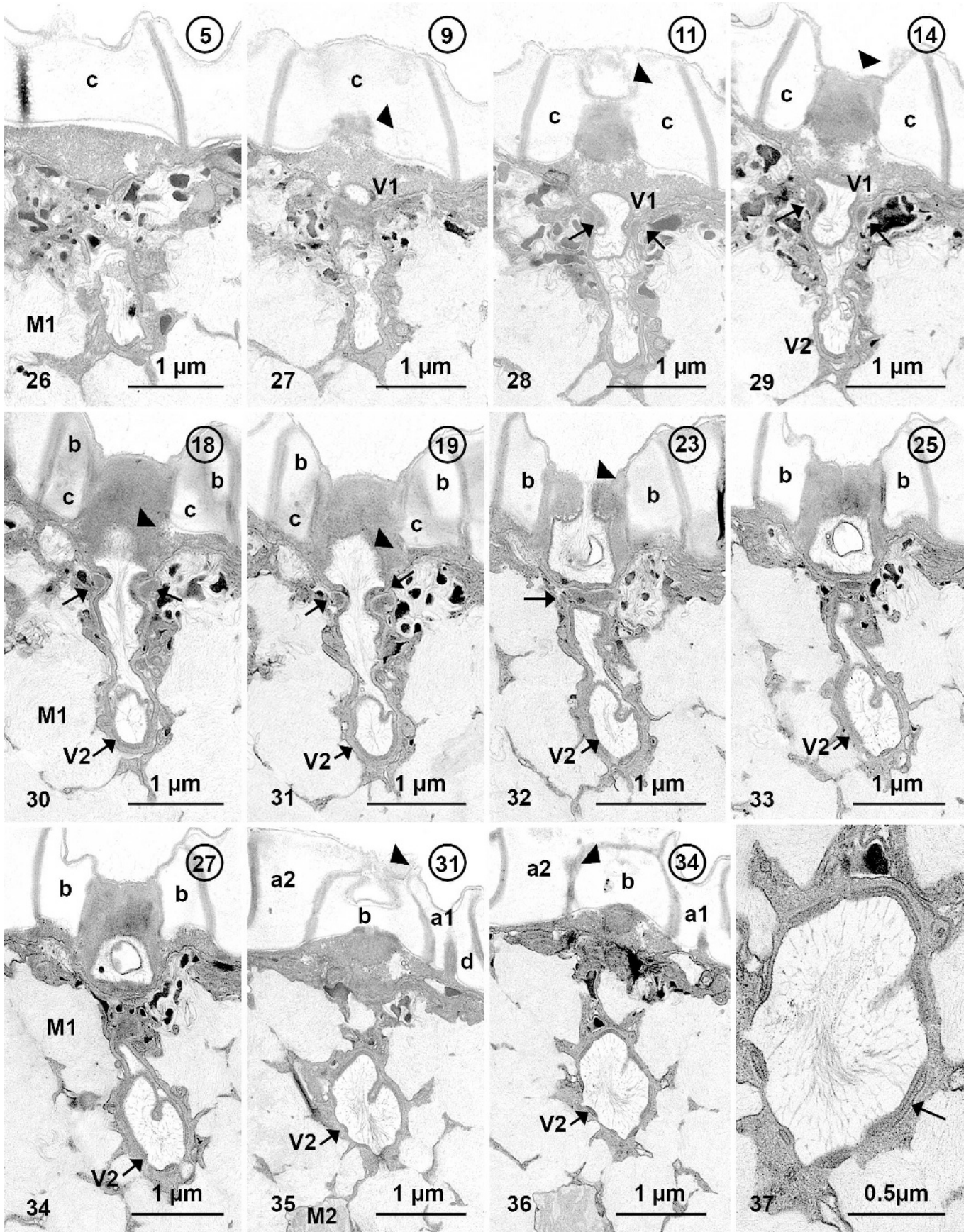
→

Figs 26–37. Selected sections from a series of sections through the periflagellar area showing the connection between the organelle resembling a pusule and the accessory pore of *Prorocentrum concavum* (syn. *P. arabianum*, CCMP 1724). The direction of sectioning is from right to the left. Small encircled numbers refer to the section number. For labelling of plates, see Fig. 25. The pusule canal is surrounded by numerous mucus vesicles (M1 and M2).

Figs 26–29. The pusule system seems to be composed of a proximal chamber, a canal and an anterior chamber, V1. The anterior chamber is at its base surrounded by a circular ring or collar (arrows).

Figs 30–33. The pusule system discharges its contents through a narrow opening between the two sac-like structures (arrowheads). A small collar surrounds V1 (arrows). The posterior chamber, V2, is located at the posterior end.

Figs 34–37. The posterior chamber, V2, is surrounded by three membranes (arrow) and contains fibrous material.



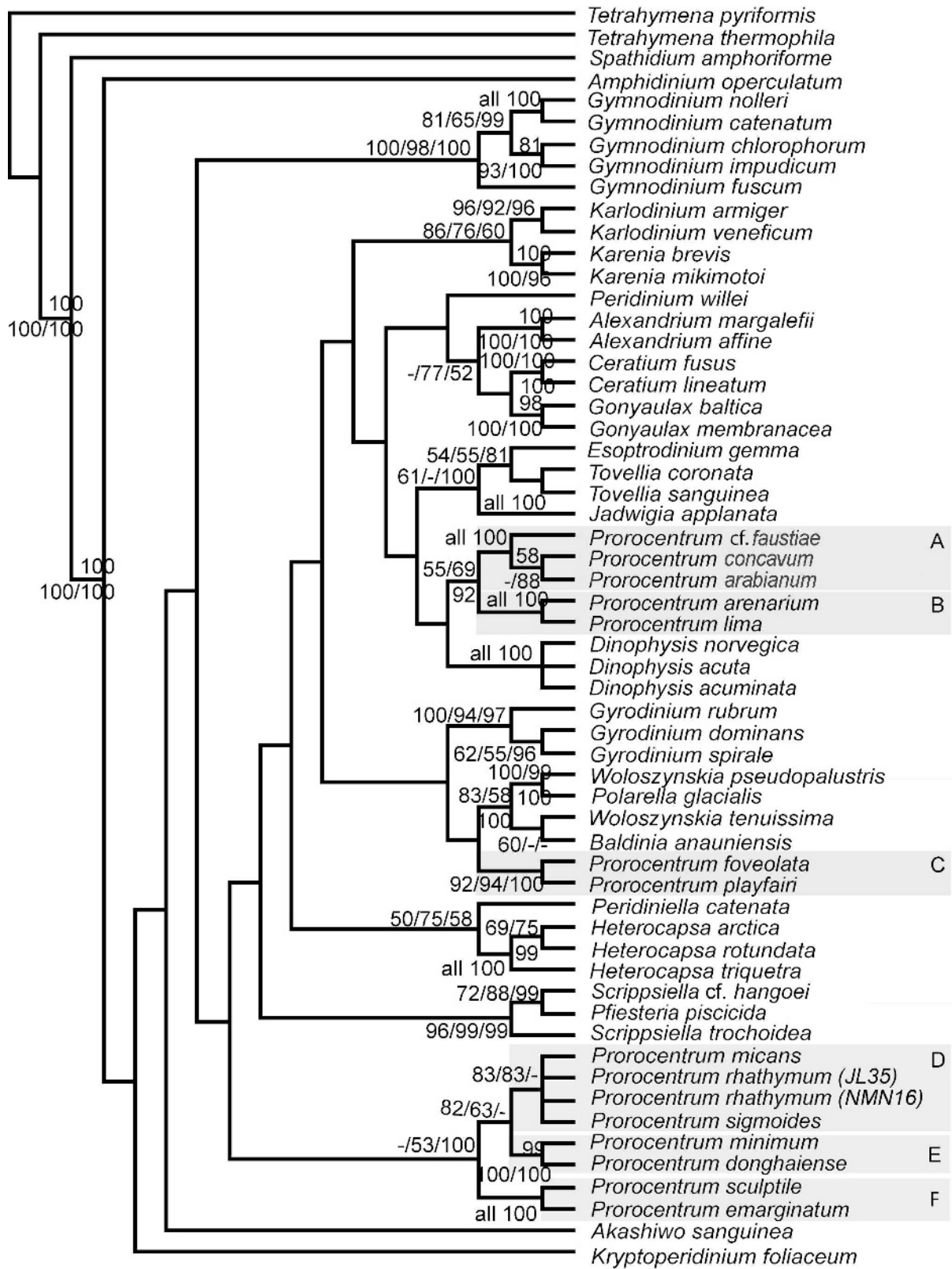


Fig. 38. Phylogeny of *Prorocentrum concavum* (NMN08), *Prorocentrum concavum* (syn. *P. arabianum*, CCMP 1724) and 53 other dinoflagellates (including 11 other species of *Prorocentrum*) based on nuclear-encoded, partial LSU rDNA sequences. The tree shown is a strict consensus of 12 equally parsimonious trees; each is 3137 steps long (CI = 0.404 and RI = 0.537). It was obtained from maximum parsimony analyses with 1000 random additions, and characters were unordered and weighted equally. Bootstrap values or support from posterior probabilities of $\geq 50\%$ are added to the left of internal nodes. Numbers from MP bootstrap (1000 replications) are written first, and numbers from neighbor-joining analyses based on maximum likelihood settings obtained from Modeltest, also with 1000 replications,

other by only one platelet (platelet c) (Figs 14, 18–22, 24, 25).

From serial sections of the periflagellar area, a structure resembling a pusule was observed to connect to the accessory pore (Figs 26–36). It is formed by a canal, bounded by two membranes (not shown) and contains fibrous material, most likely mucus (Figs 26–36). The canal is extended to form two vesicles or chambers, one at the anterior (V1) (Figs 27–29) and the other at the posterior end (V2) (Figs 29–36). V2 is surrounded by three membranes (Fig. 37). The pusule-like system is probably involved in excreting mucus through the narrow opening between the two sac-like structures (Fig. 32), which form the accessory pore. A collar was present at the base of the anterior chamber and most likely functions in regulating the activity of the pusule (Figs 28–32) as a sphincter.

Phylogeny of *Prorocentrum* based on partial LSU rDNA

The tree topology from MP analysis is shown in Fig. 38. This branching pattern did not differ significantly when compared to tree topologies obtained by NJ and Bayesian analyses (not shown). The terminal branches were relatively well supported in terms of bootstrap values and posterior probabilities. Here terminal branches represent different systematic levels (e.g. orders [Gonyaulacales], families [Kareniaceae, Tovelliaceae] and genera [*Gymnodinium*, *Dinophysis*, *Gyrodinium*]). The branching pattern for the deepest lineages received no statistical support, and therefore these branches formed a large polytomy in the bootstrap and Bayesian analyses (not shown). Despite lack of support for the deepest branches, the LSU rDNA gene suggests that the genus *Prorocentrum* is polyphyletic. The MP, NJ and Bayesian analyses indicate that the prorocentroids form at least three lineages, all fairly well supported in terms of bootstrap values and posterior probabilities. These can be further divided into six strongly supported (monophyletic) groups marked A–F in Fig. 38. Groups A and B contain five epibenthic or tycho planktonic species of *Prorocentrum* (*P. cf. faustiae*, *P. concavum*, *P. arabianum*, *P. lima* and *P. arenarium*) with a small collar in the periflagellar area, and all but *P. concavum* lack trichocysts. *Prorocentrum lima* and *P. arenarium* (group B) have a smooth valve surface, whereas species in group A have a rugose valve surface (Table 2, Fig. 38). Group C comprises the two freshwater/brackish water species (*P. foveolata* and *P. playfairi*), which have a valve surface with distinct poroids and an apical notch in the periflagellar area (Table 2, Fig. 38). As mentioned by Moestrup & Daugbjerg (2007), *P. foveolata* is almost certainly a synonym of *Haplodinium antjoliense* Klebs 1912.

Groups D and E are true planktonic to tycho planktonic species, but group D contains species with smooth to rugose valve surfaces and a distinct pattern in the valve pore arrangement (Table 2, Fig. 38). In group E, the valve

surface is covered by numerous short broad spines, and the valve pores are scattered. The periflagellar area of group D is ornamented with a distinct spine or flange, whereas in group E it comprises a few teeth/forks. The two species in group F have a different valve surface (smooth and rugose) but share a similar distinct pattern in the arrangement of valve pores and flanges on the periflagellar area (Table 2, Fig. 38).

LSU rDNA sequence divergence of group A comprising *P. arabianum* and group B

The sequence divergence estimates from the pairwise comparisons of the LSU rDNA gene revealed a difference of 0.2% between *Prorocentrum arabianum* and *P. concavum* (Table 3). The difference between these two *Prorocentrum* species and *P. cf. faustiae* was only slightly higher, 0.6–0.7%, depending on the method used to estimate the sequence divergence (Table 3). The sequence divergence between these three species of *Prorocentrum* (group A) and the closest sister group comprising *P. lima* and *P. arenarium* (group B) ranged between 16.4 and 19.8% (Table 3). The LSU rDNA sequences for *P. lima* and *P. arenarium* differ by only 3%.

DISCUSSION

A detailed morphological reexamination of the original culture of *P. arabianum* has shown that several new characters need to be added to the original description. Firstly, the cell shape varies from asymmetrical to symmetrical, elongate to broadly elongate; secondly, there are two different types of pores on the valves; thirdly, marginal pores are absent; and, finally, there are nine platelets in the periflagellar area. The variation in cell shape may be an artifact since the clone has been in culture for more than 10 years (isolated in June 1995) (Morton *et al.* 2002). Variation in cell shape has been reported also in *P. lima* (Faust 1991), and this feature is therefore not always reliable for species identification. The presence of two different pore types is not mentioned in the original description but is clearly visible in fig. 6 of Morton *et al.* (2002). The morphology of this species is very close to the benthic species *P. concavum* and *P. faustiae* (Table 4). Cells of *Prorocentrum arabianum* are more or less elongate symmetrical to asymmetrical, possess a periflagellar area with nine platelets, produce cytotoxic and ichthyotoxic compounds and are planktonic. *Prorocentrum concavum* is benthic, produces three diol esters of okadaic acid (Hu *et al.* 1993) and an ichthyotoxin (Yasumoto *et al.* 1987) and it has only eight platelets (Fukuyo 1981; Faust 1990). *Prorocentrum faustiae* is also benthic, produces okadaic acid and has 16 platelets in the periflagellar area according to Morton (1998). The number of platelets in *P. concavum* and *P.*

←

are written next. The last numbers are posterior probabilities originating from Bayesian analyses. Three ciliates (*Spathidium amphoriforme*, *Tetrahymena pyriformis* and *T. thermophila*) constitute the outgroup. Sequences determined in this study are marked in bold face. See Table 2 for an explanation of the groups of *Prorocentrum* labelled A through F.

Table 2. Comparison of the six groups (groups A–F) of *Prorocentrum* spp. derived from partial LSU rDNA.

Characters	Group A	Group B	Group C	Group D	Group E	Group F
	(<i>P. concavum</i> , <i>P. cf. faustiae</i>)	(<i>P. lima</i> , <i>P. arenarium</i>)	(<i>P. playfairi</i> , <i>P. foveolata</i>)	(<i>P. micans</i> , <i>P. rhathymum</i> , <i>P. sigmoides</i>)	(<i>P. minimum</i> , <i>P. donghaiense</i>)	(<i>P. sculptile</i> , <i>P. emarginatum</i>)
Occurrence in the water column	Epibenthic/tychoplanktonic	Epibenthic	Planktonic/semiplanktonic	Planktonic/tychoplanktonic	Planktonic	Epibenthic/benthoplanktonic
Toxins	Okadaic acid	Okadaic acid	No	Yes, but not okadaic acid	Yes, but not okadaic acid	Unknown
Trichocysts	No ¹	No	Yes	Yes	Yes	Yes
Valve surface micromorphology	Rugose	Smooth	Poreoids	Smooth/depressions	Small broad spines	Smooth/shallow depressions
Valve pore arrangement	Many pores scattered except in the centre	Many pores scattered except in the centre	Few scattered pores	Distinct pattern/scattered pores	Scattered pores	Distinct pattern
Shape of periplagellar area	Triangular shape	Triangular shape	Apical notch	Small indentation	Small indentation	Narrow V-shaped
Ornamentations of the periplagellar area	Small collar	Small collar	No ornamentation	Apical spine/flange	Tooths/forks	Flange
Habitat	Marine	Marine	Freshwater to brackish water	Marine	Marine	Marine

¹ *Prorocentrum concavum* has been seen in SEM to possess trichocysts (Mohammad-Noor *et al.* 2007).

faustiae has not been confirmed by ultrastructural studies, but the periplagellar area of *P. concavum* has been dissected under the light microscope by Fukuyo (1981). Marginal pores are absent in *P. concavum* but present in *P. faustiae*.

Generally, the ultrastructure of *P. arabianum* is similar to other *Prorocentrum* species [e.g. *P. lima* (Ehrenberg) Dodge and *P. maculosum* Faust (Zhou & Fritz 1993)]. *Prorocentrum arabianum* has two central pyrenoids as in *P. lima*, *P. maculosum* (Zhou & Fritz 1993), *P. nux* (Puigserver & Zingone 2002) and *P. emarginatum* Fukuyo (N. Mohammad-Noor, personal observation). The two pyrenoids are encircled by starch grains. This type of pyrenoid has also been reported in *P. lima* and *P. maculosum* (Zhou & Fritz 1993) but not in *P. nux* (Puigserver & Zingone 2002) and *P. emarginatum* (N. Mohammad-Noor, personal observation). Mucocysts containing a paracrystalline structure as in *P. lima* and *P. maculosum* (Zhou & Fritz 1993) were not observed in *P. arabianum*. In *P. arabianum*, the numerous vesicles (M1 and M2) containing fibrous materials are probably associated with mucus production. The contents of the vesicles differed but whether the differences between M1 and M2 are real is unknown. One may speculate that the vesicles are at different stages of maturation. It is also not clear how these vesicles empty although the most likely way is through the thecal pores. Trichocysts are lacking in *P. arabianum*, a feature seen also in the benthic *P. lima* and *P. maculosum* but not in the planktonic *P. micans*, *P. obtusidens* Schiller, *P. triestinum* Schiller, *P. marinum* (Cienkowski) Loeblich, *P. balticum* (Lohmann) Loeblich, *P. pusillum* (Schiller) Loeblich, *P. minimum* (*P. mariae-lebouriae*) (Dodge & Bibby 1973) and *P. nux* (Puigserver & Zingone 2002). A decade ago McLachlan *et al.* (1997) suggested splitting of the genus *Prorocentrum* and reinstating the genus *Exuviaella* to comprise primarily benthic species. *Exuviaella* lacks an obvious apical spine or tooth, possesses mucocysts rather than trichocysts and produces DSP-type toxins. *Prorocentrum arabianum* has a mixture of characters of the two genera: it is planktonic, lacks an obvious apical spine or tooth, lacks trichocysts and produces one cytotoxic and one ichthyotoxic compound (Morton *et al.* 2002). Overlapping characteristics have also been demonstrated in several other *Prorocentrum* species, such as benthic *P. faustiae* (Morton 1998) and *P. emarginatum* (N. Mohammad-Noor, personal observation), planktonic *P. nux* (Puigserver & Zingone 2002) and the freshwater/brackish water species *P. playfairi* and *P. foveolata* (Pearce & Hallegraeff 2004). *Prorocentrum faustiae* produces okadaic acid and DTX-1, but it lacks mucocyst pores, while *P. emarginatum* possesses both trichocysts and mucocyst-like organelles. *Prorocentrum nux* has trichocysts but lacks a conspicuous apical spine or tooth. Genetic evidence (LSU rDNA) indicates that the two freshwater species are more closely related to the benthic than to the planktonic species, despite the lack of DSP-type toxins.

Platelets

The number of platelets in the periplagellar area has been considered as one of the key characters in separating *Prorocentrum* species (Fukuyo 1981; Faust 1993a, b, 1997; Morton 1998; Ten-Hage *et al.* 2000b). Unfortunately, the

Table 3. Sequence divergence (in percentage) for five species of *Prorocentrum* based on 1349 base pairs of nuclear-encoded LSU rDNA. PAUP* (ver. 4b10) was used to estimate uncorrected ('p') distances (above diagonal). Distances given below the diagonal are based on the Kimura-2-parameter model. All nucleotide sequences were determined in this study. Strain numbers are given in parentheses.

	<i>P. arabianum</i> (CCMP 1724)	<i>P. concavum</i> (NMN08)	<i>P. cf. faustiae</i> (NMN013)	<i>P. lima</i> (NMN07)	<i>P. arenarium</i> (K-0625)
<i>P. arabianum</i>	—	0.2	0.7	17.1	16.5
<i>P. concavum</i>	0.2	—	0.6	17.1	16.5
<i>P. cf. faustiae</i>	0.7	0.6	—	17.1	16.4
<i>P. lima</i>	19.8	19.8	19.6	—	3.0
<i>P. arenarium</i>	18.9	18.9	18.8	3.0	—

number is difficult to determine correctly because of the minute size of the platelets. We have therefore determined the number and arrangement of the platelets by serial sectioning for TEM.

In *P. arabianum*, we found nine platelets and two sac-like structures surrounding each flagellar and accessory pore. A comparison with Taylor's scheme showed that *P. arabianum* has one extra platelet, a2, between a1, b and e, while the other platelets agree with Taylor's scheme. The presence of one platelet (platelet c) between the flagellar pore and the accessory pore supports the idea that this is a conservative feature, as suggested by Taylor (1980). It was also reported in *P. minimum* (*P. mariae-lebouriae*) (Loeblich 1976) and *P. nux* (Puigserver & Zingone 2002), while *P. emarginatum* possesses two platelets in this area (N. Mohammad-Noor, personal observation). No obvious ornamentation such as a flange or spine was found in *P. arabianum*. A small apical collar was observed to partly surround the flagellar pore, and this collar extends from platelets c and g. In other *Prorocentrum* species, ornamentation such as spines, teeth, flanges or collars have been reported to extend from platelets a (Taylor 1980; Honsell & Talarico 1985), c, e and f (Honsell & Talarico 1985). Platelet b, which is located between a1, a2, c, d and e, is difficult to see in SEM and may be confused with the accessory pore. The number of platelets reported in other species of *Prorocentrum* is based mostly on SEM and has been found to vary from five to six in *P. formosum* (Faust 1993b); seven in *P. foveolata* Croome & Tyler (Croome & Tyler 1987), *P. elegans* Faust (Faust 1993a) and *P. nux* (Puigserver & Zingone 2002); eight in *P. lima* (Fukuyo 1981), *P. playfairi* Croome & Tyler (Croome & Tyler 1987), *P. concavum* (Fukuyo 1981), *P. maculosum*, *P. foraminosum* Faust (Faust 1993b), *P. norrisianum* Faust & Morton and *P. tropicalis* Faust (Faust 1997); and to no less than 16 in *P. faustiae* (Morton 1998). However, more detailed studies on the periflagellar area, preferably using TEM, are required to confirm these numbers and to understand the configuration of the platelets before it can be used as a solid taxonomic character. So far, the arrangement of platelets in species of *Prorocentrum* is uniform (this study; Faust 1974; Loeblich 1976; Taylor 1980; Honsell & Talarico 1985; Puigserver & Zingone 2002), and these may in the future have a potential to be used to infer the relationship between *Prorocentrum* species.

Periflagellar area

Two different-sized pores penetrate the periflagellar area. In *P. arabianum*, both flagella emerge from the flagellar pore,

the largest pore, as also reported previously in other species (Loeblich *et al.* 1979; Honsell & Talarico 1985; Zhou & Fritz 1993; Roberts *et al.* 1995). The smaller pore is known by several names but the most widely used term is auxiliary pore (e.g. Honsell & Talarico 1985; Faust 1993a, b; Morton 1998; Faust *et al.* 1999; Puigserver & Zingone 2002). Although the existence of this pore is well established, its function is still unknown. Several researchers have suggested that the pore is associated with the pusule (Fensome *et al.* 1993) and may be involved in mucilage excretion (Loeblich *et al.* 1979; Steidinger & Tangen 1996), while others have suggested a role in attachment of the cell (Steidinger & Tangen 1996). In this study we have reported a connection between a pusule-like organelle and the small pore, indicating that the term 'accessory pore' is more appropriate. Auxiliary means 'helping' and is meaningless in this connection. Apical pore is also inappropriate, as it is used to describe a large pore or series of pores located at the apex of the episome of other dinoflagellates (Fensome *et al.* 1993). Previous studies of *Prorocentrum* species have shown that the pusule is positioned at the base of either the flagellar pore or the accessory pore. In *P. lima* and *P. maculosum*, it is most likely situated below the accessory pore (Zhou & Fritz 1993, p. 448, figs 9, 11). Figure 9 must be interpreted with caution because of the possible displacement of plates in the periflagellar area, which may have caused both the flagellar pore and the accessory pore to shift to the left. In *P. nux* (Puigserver & Zingone 2002) and *P. micans* (Roberts *et al.* 1995), the pusule was reported to be situated near the flagellar bases. This discrepancy, however, may be caused by the presence of more than one pusule in *Prorocentrum*. Thus, two pusules have been reported in *P. micans* (Schütt 1895; Roberts *et al.* 1995), and one of the pusules opens into the flagellar canal (Roberts *et al.* 1995). In *P. arabianum*, only one pusule-like organelle was observed, and the same applies to *P. lima*, *P. maculosum* (Zhou & Fritz 1993) and *P. nux* (Puigserver & Zingone 2002). In other dinoflagellates, the presence of one (Steidinger *et al.* 1978) or two pusules has also been reported, each pusule associating with a flagellar canal (e.g. Hansen *et al.* 1996; Leadbeater & Dodge 1966; Hansen & Moestrup 1998; Calado *et al.* 1999; Hansen *et al.* 2000b).

The organelle resembling a pusule in *P. arabianum* is surrounded by two membranes, contains fibrous material and comprises a canal with two vesicles, one at the anterior (V1) and the other at the posterior end (V2). V2 appears to be associated with numerous mucus vesicles (M1 and M2) at the posterior end. This pusule is similar to that reported in *P. lima* and *P. maculosum* in content and number of

Table 4. Comparison of *Prorocentrum arabianum* with the original description by Morton *et al.* (2002), *P. concavum* (Fukuyo 1981; Yasumoto *et al.* 1987; Faust 1990; Hu *et al.* 1993; Faust *et al.* 1999; Mohammad-Noor *et al.* 2007) and *P. faustiae* (Morton, 1998).

Characteristics	<i>P. arabianum</i> (this study)	<i>P. arabianum</i> (original description)	<i>P. concavum</i>	<i>P. faustiae</i>
Cell size (µm), DV: dorsoventral W: width	DV: 38-49 W: 35-40 (<i>n</i> = 20)	DV: 42-48, W: 35-40 (<i>n</i> = 22)	DV: 44-45, LR: 40; DV: 50-55, W: 38-45 DV: 43-53, W: 38-48	DV: 43-49, W: 38-42 (<i>n</i> = 50)
Cell shape	Broadly elongate, symmetrical or asymmetrical	Broadly oval, asymmetrical in valve view, maximum width behind the middle region	Broadly ovate	Broadly ovate to rotundate
Thecal surface	Rugose	Rugose	Areolated	Rugose
Valve pores (µm) Lp: large pore Sp: small pore D: diameter	Two different type of pores situated in shallow depressions, Lp: 0.17-0.21 Sp: 0.10-0.13	Small pores situated in round shallow depressions D: 0.12 µm (<i>n</i> = 10)	Two different sizes of pores situated in shallow depressions D: 0.12-0.23	Small pores, D: 0.1 µm
Marginal pores	Absent	Not known	Absent	Present
Periflagellar area	Broad V-shaped, small collar	V-shaped depression, no ornamentation	Narrow triangular, no ornamentation	Wide triangle, no ornamentation
No. of platelets	9 platelets	Not known	8 platelets	16 platelets
Intercalary band	Horizontally striated	Smooth and horizontally striated	Horizontally striated	Horizontally striated
Pyrenoid	Two and centrally located	Present	Centrally located	Centrally located
Toxin	Not tested	One cytotoxic and one ichthyotoxic compound	3 diol ester of okadaic acid and ichthyotoxin	Okadaic acid and DTX-1
Mode of living/swimming	Not an active swimmer, produces conspicuous amount of mucilage	Planktonic, motile, swims freely	Benthic, motile or embedded in mucus	Benthic

membranes surrounding the pusule (Zhou & Fritz 1993, p. 448, figs 9, 11). Dodge (1972) suggested that *Prorocentrum* has a sac-type pusule, and this type has been reported recently in *P. nux* (Puigserver & Zingone 2002). However, we did not observe this type in *P. arabianum*, nor was it found in *P. lima* and *P. maculosum* (Zhou & Fritz 1993). The pusule canal contained fibrous material that appeared to be in the process of being discharged through the small pore between the two opaque structures. The organelle therefore seems to be an exit route for mucus or other particulate matter. Studies on the structure and function of the pusule in *P. micans* and *Amphidinium carterae* Hulbert have suggested that the pusule is a multifunction organelle used in osmoregulation, macromolecule uptake and secretion (Klut *et al.* 1987). The small collar surrounding the pusule canal in *P. arabianum* is most likely a means of controlling the secretion of the contents. Roberts *et al.* (1995) reported the presence of a striated collar around the accessory pore in *P. micans*, and the pore was associated with two different types of vesicle (mucocysts and fibrous vesicles). This striated collar may be homologous with the collar observed in *P. arabianum*. In other dinoflagellates, such as in *Peridinium cinctum* (O. F. Müller) Ehrenberg, striated collars have been suggested to be responsible for changes in pusular volume (Calado *et al.* 1999). However, the studies on the pusule in *Prorocentrum* species are still inconclusive and do not allow definite conclusions on its structure and function.

Systematics of *P. arabianum* and phylogeny of *Prorocentrum*

The LSU rDNA sequences determined here suggest that the original material used to describe *P. arabianum* and *P. concavum* isolated from Malaysian waters are conspecific, as the LSU rDNA sequence divergence was only 0.2%. Such a low sequence divergence is usually seen only at the population level (e.g. Hansen *et al.* 2000a). To further elucidate the likely conspecificity of *P. arabianum* and *P. concavum*, we determined a more variable fragment of DNA (ITS 1 and ITS 2) in addition to a gene from a separate genetic compartment, the mitochondrial cytochrome *b* gene. The latter two DNA fragments were identical (ITS) or almost identical (cob) in the two strains, providing strong molecular evidence for conspecificity between *P. arabianum* and *P. concavum*. Hence, the molecular sequence data from three different DNA fragments (two separate genetic compartments) in combination with the subtle morphological differences therefore lead us to conclude that *P. arabianum* (Morton & Faust 2002) and *P. concavum* Fukuyo are identical and *P. arabianum* therefore a synonym of *P. concavum*. It should be noted that the LSU rDNA sequence from the Malaysian isolate of *P. concavum* is nearly identical (four substitutions out of 893 base pairs in the comparison) to a sequence from an isolate from Réunion determined by C. X. Pochon and coworkers and available in GenBank (accession number AJ567464).

The phylogenetic analyses based on partial LSU rDNA did not provide strong support for the divergent dinoflagellate lineages. Even so, the diverse assemblage of *Prorocentrum* with 13 species included did not cluster as

a single well-supported monophyletic clade but rather appeared as a number of distinct evolutionary groups (Fig. 38). Based on habitat, morphological characters and production of okadaic acid (see Table 2), *Prorocentrum* was divided into six groups (A through F) each fairly well supported in terms of bootstrap support or posterior probabilities. Despite little or no statistical support from the molecular analyses, the LSU rDNA sequences in combination with morphology indicate that the genus *Prorocentrum sensu lato* is heterogeneous and may eventually be divided into a number of genera. However, studies of additional *Prorocentrum* species are required, and these should include nucleotide sequence data from new genes (i.e. nonribosomal).

ACKNOWLEDGEMENTS

We thank Lisbeth Haukrogh for TEM assistance and Charlotte Hansen for running the cycle sequencing reactions. We acknowledge Statens Naturhistoriske Museum, Copenhagen, for letting us use their DNA sequencing facility. Robert A. Andersen kindly provided the CCMP culture of *P. arabianum*, and Gert Hansen is thanked for suggestions to improve the manuscript. N.D. thanks Miguel de Salas and Imojen Pearce (University of Tasmania) for additional LSU rDNA sequence data from *P. playfairi* and *P. foveolata*. N.M-N. was supported by a Ph.D. scholarship awarded by the Public Services Department, Malaysia, and Universiti Malaysia Sabah. This study was also supported by the Danish Science Research Council (project #21-02-0539 to ØM and ND) and the Carlsberg Foundation (project #ANS-1613/40 to ND).

REFERENCES

BIECHELER B. 1952. Recherches sur les Péridiniens. *Bulletin Biologique de la France et de la Belgique*. Supplement 36: 20–22.

BURSA A. 1959. The genus *Prorocentrum* Ehrenberg. Morphodynamics, protoplasmatic structures and taxonomy. *Canadian Journal of Botany* 37: 1–30.

CALADO A.J., HANSEN G. & MOESTRUP Ø. 1999. Architecture of the flagellar apparatus and related structures in the type species of *Peridinium*, *P. cinctum* (Dinophyceae). *European Journal of Phycology* 34: 179–191.

CROOME R.L. & TYLER P.A. 1987. *Prorocentrum playfairi* and *Prorocentrum foveolata*, two new dinoflagellates from Australian freshwater. *British Phycological Journal* 22: 67–75.

DAUGBJERG N., HANSEN G., LARSEN J. & MOESTRUP Ø. 2000. Phylogeny of some of the major genera of dinoflagellates based on ultrastructure and partial LSU rDNA sequence data, including the erection of three new genera of unarmoured dinoflagellates. *Phycologia* 39: 302–317.

DENARDOU-QUENEHERVE A., GRZEBYK D., POUCHUS Y.F., SAUVIAT M.P., ALLIOT E., BIARD J.F., BERLAND B. & VERBIST J.F. 1999. Toxicity of French strains of the dinoflagellate *Prorocentrum minimum* experimental and natural contaminations of mussels. *Toxicon* 37: 1711–1719.

DE RIJK, P., WUYTS J., VAN DER PEER, Y., WINKELMANS T. & DE WACHTER, R. 2000. The European large subunit ribosomal RNA database. *Nucleic Acids Research* 28: 117–118.

DODGE J.D. 1972. The ultrastructure of the dinoflagellate pusule: a unique osmo-regulatory organelle. *Protoplasma* 75: 285–302.

DODGE J.D. & BIBBY B.T. 1973. The Prorocentrales (Dinophyceae) I. A comparative account of fine structure in the genera *Prorocentrum* and *Exuviaella*. *Botanical Journal of the Linnean Society* 67: 175–187.

DOYLE J. & DOYLE J. 1987. A rapid DNA isolation procedure for small quantities of fresh leaf tissue. *Phytochemistry Bulletin* 19: 11–15.

FAUST M.A. 1974. Micromorphology of a small dinoflagellate *Prorocentrum mariae-lebouriae* (Parke & Ballatine) comb. nov. *Journal of Phycology* 10: 315–322.

FAUST M.A. 1990. Morphology details of six benthic species of *Prorocentrum* (Phytophyta) from a mangrove island, Twin Cays, Belize, including two new species. *Journal of Phycology* 26: 548–558.

FAUST M.A. 1991. Morphology of ciguatera-causing *Prorocentrum lima* (Pyrophyta) from widely differing sites. *Journal of Phycology* 27: 642–648.

FAUST M.A. 1993a. *Prorocentrum belizeanum*, *Prorocentrum elegans* and *Prorocentrum caribbaeum*, three new benthic species (Dinophyceae) from a mangrove island, Twin Cays, Belize. *Journal of Phycology* 29: 100–107.

FAUST M.A. 1993b. Three new benthic species of *Prorocentrum* (Dinophyceae) from Twin Cays, Belize: *P. maculosum* sp. nov., *P. foraminosum* sp. nov. and *P. formosum* sp. nov. *Phycologia* 32: 410–418.

FAUST M.A. 1994. Three new benthic species of *Prorocentrum* (Dinophyceae) from Carrie Bow Cay, Belize: *P. sabulosum* sp. nov., *P. sculptile* sp. nov., and *P. arenarium* sp. nov. *Journal of Phycology* 30: 755–763.

FAUST M.A. 1997. Three new benthic species of *Prorocentrum* (Dinophyceae) from Belize: *P. norrisianum* sp. nov., *P. tropicalis* sp. nov., and *P. reticulatum* sp. nov. *Journal of Phycology* 33: 851–858.

FAUST M.A., LARSEN J. & MOESTRUP Ø. 1999. Potentially toxic phytoplankton. 3. Genus *Prorocentrum* (Dinophyceae). In: *ICES Identification Leaflets for Plankton* (Ed. by J.A. Lindley), pp. 1–23. International Council for the Exploration of the Sea, Copenhagen.

FENSOME R.A., TAYLOR F.J.R., NORRIS G., SARJEANT W.A.S., WHARTON D.I. & WILLIAMS G.L. 1993. A classification of living and fossil dinoflagellates. *Micropaleontology* Special Pub. No. 7, pp. 158–159.

FRITZ L. & TRIEMER R.E. 1985. A rapid technique utilizing calcofluor white M2R for the visualization of the dinoflagellate thecal plates. *Journal of Phycology* 21: 662–664.

FUKUYO Y. 1981. Taxonomical study on benthic dinoflagellates collected in corals reefs. *Bulletin of the Japanese Society of Scientific Fisheries* 47: 967–978.

GALTIER N., GOUY M. & GAUTIER C. 1996. SeaView and Phylo_win, two graphic tools for sequence alignment and molecular phylogeny. *Computer Applications in the Biosciences* 12: 543–548.

GUILLARD R.R.L. & HARGRAVES P.E. 1993. *Stichochrysis immobilis* is a diatom, not a chrysophyte. *Phycologia* 32: 234–236.

HANSEN G. & DAUGBJERG N. 2004. Ultrastructure of *Gyrodinium spirale*, the type species of *Gyrodinium* (Dinophyceae), including a phylogeny of *G. dominans*, *G. rubrum* and *G. spirale* deduced from partial LSU rDNA sequences. *Protist* 155: 271–294.

HANSEN G. & MOESTRUP Ø. 1998. Light and electron microscopical observations on *Peridiniella catenata* (Dinophyceae). *European Journal of Phycology* 33: 293–305.

HANSEN G., MOESTRUP Ø. & ROBERTS K.R. 1996. Fine structural observations on *Gonyaulax spinifera* (Dinophyceae), with special emphasis on the flagellar apparatus. *Phycologia* 35: 354–366.

HANSEN G., DAUGBJERG N. & HENRIKSEN P. 2000a. Comparative study of *Gymnodinium mikimotoi* and *Gymnodinium aureolum* comb. nov. (*Gyrodinium aureolum*) based on morphology, pigment composition and molecular data. *Journal of Phycology* 36: 394–410.

HANSEN G., MOESTRUP Ø. & ROBERTS K.R. 2000b. Light and electron microscopical observations on the type species of *Gymnodinium*, *G. fuscum* (Dinophyceae). *Phycologia* 39: 365–376.

- HOLMES M.J., LEE F.C., KHOO H.W. & TEO S.L.M. 2001. Production of 7-deoxy-okadaic acid by a New Caledonian strain of *Prorocentrum lima* (Dinophyceae). *Journal of Phycology* 37: 280–288.
- HONSELL G. & TALARICO L. 1985. The importance of flagellar arrangement and insertion in the interpretation of the theca of *Prorocentrum* (Dinophyceae). *Botanica Marina* 28: 15–21.
- HOPPENRATH M. 2000. A new marine sand-dwelling *Prorocentrum* species, *P. clipeus* sp. nov. (Dinophyceae, Prorocentrales) from Helgoland, German Bight, North Sea. *European Journal of Protistology* 36: 29–33.
- HU T., DEFREITAS A.S.W., DOYLE J., JACKSON D., MARR J., NIXON E., PLEASANCE S., QILLIAM M.A., WALTER A. & WRIGHT J.L.C. 1993. New DSP toxin derivatives isolated from toxic mussels and the dinoflagellates, *Prorocentrum lima* and *Prorocentrum concavum*. In: *Toxic Phytoplankton Blooms in the Sea* (Ed. by T.J. Smayda & Y. Shimizu), pp. 507–512. Elsevier Science Publishers, New York.
- KLEBS G. 1912. Über Flagellaten- und Algen-ähnlichen Peridineen. *Verhandlungen des Naturhistorisch-Medizinischen Vereines zu Heidelberg*, Neue Folge 11: 369–451.
- KLUT M.E., BISALPUTRA T. & ANTIA N.J. 1987. Some observations on the structure and function of the dinoflagellate pusule. *Canadian Journal of Botany* 65: 736–744.
- KOFOID A. & SWEZY O. 1921. *The free-living unarmored dinoflagellata*. Memoirs of the University of California. University of California Press, Berkeley. Vol. 5: 1–562.
- KOKINOS J.P. & ANDERSON D.M. 1995. Morphological development of resting cysts in cultures of the marine dinoflagellate *Lingulodinium polyedrum* (= *L. machaerophorum*). *Palynology* 19: 143–166.
- LEADBEATER B. & DODGE J.D. 1966. The fine structure of *Woloszynskia micra* sp. nov., a new marine dinoflagellate. *British Phycological Bulletin* 3: 1–17.
- LENAERS G., MAROTEAUX L., MICHOT B. & HERZOG M. 1989. Dinoflagellates in evolution: a molecular phylogenetic analysis of large subunit ribosomal RNA. *Journal of Molecular Evolution* 29: 40–51.
- LOEBLICH III A.R. 1976. Dinoflagellate evolution: speculation and evidence. *Journal of Protozoology* 23: 13–28.
- LOEBLICH III A.R., SHERLEY J.L. & SCHMIDT R.J. 1979. The correct position of flagellar insertion in *Prorocentrum* and description of *Prorocentrum rhathymum* sp. nov. (Pyrrhophyta). *Journal of Plankton Research* 1: 113–120.
- MCLACHLAN J.L., BOALCH G.T. & JAHN R. 1997. Reinstatement of the genus *Exuviaella* (Dinophyceae, Prorocentrophycidae) and assessment of *Prorocentrum lima*. *Phycologia* 36: 38–46.
- MOESTRUP Ø. & DAUGBJERG N. 2007. On dinoflagellate phylogeny and classification. In: *Unravelling the algae: the past, present, and future of algae systematics* (Ed. by J. Brodie & J.M. Lewis), Systematics Association Special Volume 75, CRC Press, Boca Raton, FL. in press.
- MOHAMMAD-NOOR N., DAUGBJERG N., MOESTRUP Ø. & ANTON A. 2007. Marine epibenthic dinoflagellates from Malaysia – a study of live cultures and preserved samples based on light and scanning electron microscopy. *Nordic Journal of Botany* 24: 629–690.
- MORTON S.L. 1998. Morphology and toxicology of *Prorocentrum faustiae* sp. nov., a toxic species of non-planktonic dinoflagellate from Heron Island, Australia. *Botanica Marina* 41: 565–659.
- MORTON S.L., MOELLER P.D.R., YOUNG K.A. & LANOUE B. 1998. Okadaic acid production from the marine dinoflagellate *Prorocentrum belizeanum* Faust isolated from the Belizean coral reef ecosystem. *Toxicon* 36: 201–206.
- MORTON S.L., FAUST M.A., FAIREY E. & MOELLER P.D.R. 2002. Morphology and toxicology of *Prorocentrum arabianum* sp. nov., (Dinophyceae) a toxic planktonic dinoflagellate from the Gulf of Oman, Arabian Sea. *Harmful Algae* 1: 393–400.
- MURAKAMI Y., OSHIMA Y. & YASUMOTO T. 1982. Identification of okadaic acid as a toxic component of a marine dinoflagellate *Prorocentrum lima*. *Bulletin of the Japanese Society of Scientific Fisheries* 48: 69–72.
- PARKE M. & BALLANTINE D. 1957. A new marine dinoflagellate: *Exuviaella mariae-lebouriae* n. sp. *Journal of Marine Biological Association U.K.* 36: 643–650.
- PEARCE I. & HALLEGRAEFF G.M. 2004. Genetic affinities, ecophysiology and toxicity of *Prorocentrum playfairii* and *P. foveolata* (Dinophyceae) from Tasmania freshwaters. *Phycologia* 43: 271–281.
- POSADA D. & CRANDALL K.A. 1998. MODELTEST: testing the model of DNA substitution. *Bioinformatics* 14: 817–818.
- PUIGSERVER M. & ZINGONE A. 2002. *Prorocentrum nux* sp. nov. (Dinophyceae), a small planktonic dinoflagellate from the Mediterranean Sea, and discussion of *P. nanum* and *P. pusillum*. *Phycologia* 41: 29–38.
- ROBERTS K.R., HEIMANN K. & WETHERBEE R. 1995. The flagellar apparatus and canal structure in *Prorocentrum micans* (Dinophyceae). *Phycologia* 34: 313–322.
- RONQUIST F. & HUELSENBECK J.P. 2003. MRBAYES 3: Bayesian phylogenetic inference under mixed models. *Bioinformatics* 19: 1572–1574.
- SCHOLIN C.A., HERZOG M., SOGIN M. & ANDERSON D.M. 1994. Identification of group- and strain-specific genetic markers for globally distributed *Alexandrium* (Dinophyceae). II. Sequence analysis of a fragment of the LSU rRNA gene. *Journal of Phycology* 30: 999–1011.
- SCHÜTT F. 1895. Die Peridineen der Plankton-Expedition. Part I. Kiel und Leipzig, Verlag von Lipsius & Tischer, pp. 45–55.
- SCHÜTT F. 1896. Gymnodiniaceae, Prorocentrales, Peridiniaceae, Bacillariaceae. In: *Die natürlichen Pflanzenfamilien* (Ed. by A. Engler & K. Prantl), 1(1), pp. 6–9.
- STEIDINGER K.A. & TANGEN K. 1996. Dinoflagellates. In: *Identifying marine diatoms and dinoflagellates* (Ed. by C.R. Tomas), pp. 387–584. Academic Press, San Diego, CA.
- STEIDINGER K.A., TRUBY E.W. & DAWES C.J. 1978. Ultrastructure of the red tide dinoflagellate *Gymnodinium breve*. I. General description. *Journal of Phycology* 14: 72–79.
- SWOFFORD D.L. 2003. PAUP* phylogenetic analysis using parsimony (*and other methods), version 4., Sinauer Associates, Sunderland, MA.
- TAYLOR F.J.R. 1980. On dinoflagellate evolution. *Biosystems* 13: 65–108.
- TEN-HAGE L., DELAUNAY N., PICHON V., COUTÉ A., PUISEUX-DAO S. & TURQUET J. 2000a. Okadaic acid production from the marine benthic dinoflagellate *Prorocentrum arenarium* Faust (Dinophyceae) isolated from Europa Island coral reef ecosystem (SW Indian Ocean). *Toxicon* 38: 1043–1054.
- TEN-HAGE L., TURQUET J., QUOD J.-P., PUISEUX-DAO S. & COUTÉ A. 2000b. *Prorocentrum borbonicum* sp. nov. (Dinophyceae), a new toxic benthic dinoflagellate from the southwestern Indian Ocean. *Phycologia* 39: 296–301.
- TEN-HAGE L., ROBILLOT C., TURQUET J., LE GALL F., LE CAER J.-P., BULTEL V., GUYOT M. & MOLGO J. 2002. Effects of toxic extracts and purified borbotoxins from *Prorocentrum borbonicum* (Dinophyceae) on vertebrate neuromuscular junctions. *Toxicon* 40: 137–148.
- WHITE T.J., BRUNS T., LEE S. & TAYLOR J. 1990. Amplification and direct sequencing of fungal ribosomal RNA genes for phylogenetics. In: *PCR protocols: a guide to methods and applications* (Ed. by M.A. Innis, D.H. Gelfand, J.J. Sninsky & T.J. White), pp. 315–322. Academic Press, San Diego, CA.
- YANG Z. & RANNALA B. 1997. Bayesian phylogenetic inference using DNA sequences: a Markov chain Monte Carlo method. *Molecular Biology and Evolution* 14: 717–724.
- YASUMOTO T., SEINO N., MURAKAMI Y. & MURATA M. 1987. Toxins produced by benthic dinoflagellates. *Biological Bulletin* 172: 128–131.
- ZHANG H., BHATTACHARYA D. & LIN S. 2005. Phylogeny of dinoflagellates based on mitochondrial cytochrome b and nuclear small subunit rDNA sequences comparisons. *Journal of Phycology* 41: 411–420.
- ZHOU J. & FRITZ L. 1993. Ultrastructure of two toxic marine dinoflagellates, *Prorocentrum lima* and *Prorocentrum maculosum*. *Phycologia* 32: 444–450.

Received 31 October 2006; accepted 14 May 2007
Associate editor: Jacob Larsen